Theoretical framework of Thomson scattering

in laser produced plasmas

Wojciech Rozmus

Department of Physics, University of Alberta

Outline

- Thomson scattering from the particle noise – form factor, 1960, for stable, collisionless plasma not necessary in thermal equilibrium.
- Form factor with particle collisions from nonlocal and nonstationary hydrodynamics
- Enhanced fluctuation levels – thermal response to incoherent laser pulses
- Non-Maxwellian distribution functions – super Gaussians in laser heated plasmas, modified by thermal transport.
- Electromagnetic, Weibel unstable plasmas – laboratory astrophysics, measurement of the magnetic fields
- Langmuir and ion acoustic turbulence – enhanced fluctuation spectra, absorption, modified transport

Fluctuations due to particle discretness

Fluctuations & Thomson scattering

Thomson scattering (TS) cross section is proportional to the dynamical form factor $S(\vec{k},\omega)$. For stable plasmas (but not necessary in equilibrium) particle discretness gives rise to electron (small amplitude) density fluctuations and their correlation function, as follows (J. Feyer, Can. J. Phys. (1960); J. Renau, J. Geophys. Res. (1960); J. Daugherty, D. Farley, Proc. Roy. Soc. (1960); E. Salpeter, Phys. Rev. (1960).

$$S(\vec{k},\omega) = \frac{\langle \delta n_e^2 \rangle_{k,\omega}}{n_e} = \frac{2\pi}{k}\left\{ \left|1-\frac{\chi_e}{\epsilon}\right|^2 f_{e0}\left(\frac{\omega}{k}\right) + \sum_{j(ions)} \frac{Z_j^2 n_j}{n_e}\left|\frac{\chi_e}{\epsilon}\right|^2 f_{j0}\left(\frac{\omega}{k}\right)\right\}, \quad n_i = \sum_j n_j$$

where linear response functions evaluated using distribution functions f_{e0}, f_{j0}, are

$$\epsilon = 1 + \chi_e + \sum_j \chi_j$$

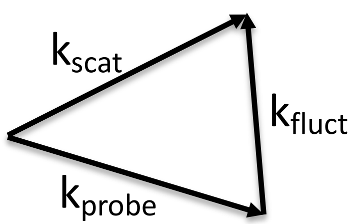

$$\omega_s = \omega_0 + \omega$$

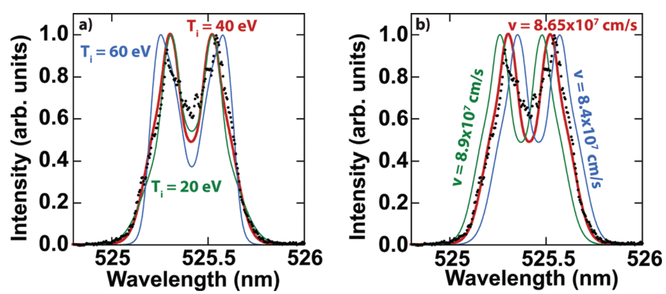

FIG. 4. The Thomson scattering cross section is fit to the measured Thomson scattering ion feature at 5.5 ns to determine the ion temperature and plasma flow velocity. The best fit to the experimental data (red line) is calculated using an electron temperature and density determined from the electron feature (100 eV and $5.6 \times 10^{18}\text{cm}^{-3}$), ion temperature of 40 eV, and a plasma flow velocity of $8.65 \times 10^7\text{cm/s}$. (a) The ion temperature is increased to 60 eV (green line) and decreased to 20 eV (blue line) to demonstrate the sensitivity of the fit. (b) The plasma flow velocity is varied from $8.9 \times 10^7\text{cm/s}$ (green line) to $8.4 \times 10^7\text{cm/s}$ (blue line) as well.

Example from the paper by S. Ross *et al*. Phys. Plasmas **19**, 056501 (2012) on interpenetrating plasmas. Two ion acoustic peaks are shown and are fitted with the $S(\vec{k},\omega)$ and Maxwellians

Effect of particle collisions

PHYSICAL REVIEW E **96**, 043207 (2017)

Electrostatic fluctuations in collisional plasmas

W. Rozmus,[1] A. Brantov,[2] C. Fortmann-Grote,[3] V. Yu. Bychenkov,[2] and S. Glenzer[4]

It is difficult to properly include collisions into calculations of $S(\vec{k},\omega)$. In this paper we have used nonlocal and nonstationary transport theory and Onsager hypothesis.

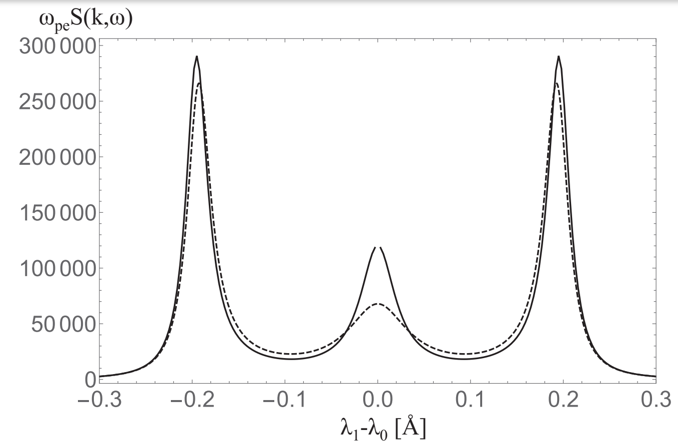

FIG. 1. Dynamical form factors for argon plasma at $n_e = 10^{17}$ cm^{-3}, $T = 2$ eV, $Z = 1$, $A = 18$. The probe wavelength is $\lambda_0 = 10.6\ \mu$m and the scattering angle $\theta = 6^\circ$. Dashed line is obtained using Eq. (54) and the continuous black line corresponds to the full theoretical $S(k,\omega)$ of our theory Eq. (51) for $T_e = T_i = T$.

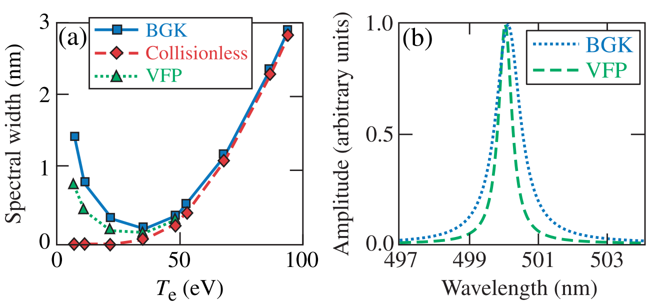

FIG. 5. (a) The width (FWHM) of the redshifted EPW features is plotted for a density of 10^{19} cm^3 using the collisionless (red diamonds), BGK (blue squares), and VFP (green triangles) models as functions of electron temperature. (b) The spectrum calculated with the BGK model (blue dashed line) and the VFP model (green dashed line) are shown for $T_e = 11$ eV and $n_e = 1.07 \times 10^{19}$ cm^3. To illustrated the width differences, the BGK spectrum was multiplied by 1.8.

PHYSICAL REVIEW LETTERS **122,** 155001 (2019)

Picosecond Thermodynamics in Underdense Plasmas Measured with Thomson Scattering

A. S. Davies,[1,2*] D. Haberberger,[1] J. Katz,[1] S. Bucht,[1,2] J. P. Palastro,[1] W. Rozmus,[3,4] and D. H. Froula[1,2]

The rapid evolutions of the electron density and temperature in a laser-produced plasma were measured using collective Thomson scattering. Unprecedented picosecond time resolution, enabled by a pulse-front-tilt compensated spectrometer, revealed a transition in the plasma-wave dynamics from an initially cold, collisional state to a quasistationary, collisionless state. The Thomson-scattering spectra were compared with theoretical calculations of the fluctuation spectrum using either a conventional Bhatnagar-Gross-Krook (BGK) collision operator or the rigorous Landau collision terms: the BGK model overestimates the electron temperature by 50% in the most-collisional conditions.

Fluctuation Dissipation Theorem

In the strongly collisional regime, $k\lambda_{\alpha\beta} \ll 1$, (cf. e.g. Zhang, et al. Phys. Rev. Lett. **62**, 1848 (1989)) classical transport relations (Braginskii, (1965)) are used to evaluate frequency dependent electrical conductivity $\sigma_e(k,\omega)$.

Fluctuation-dissipation theorem: $S(k,\omega) = \dfrac{k^2 T}{\pi \omega^2 e^2 n_e} \mathrm{Re}[\sigma_e(k,\omega)]$, directly relates $\sigma_e(k,\omega)$ to the dynamical form factor.

But plasma needs to be in thermodynamical equilibrium, $T_e = T_i = T$.

$$S(k,\omega) = 2 \frac{A(k) + B(k) b(k)/D(k,\omega)}{[A(k) + B(k) b(k)/D(k,\omega)]^2 \omega^2 + H(k,\omega)^2}$$

$$H(k,\omega) = 2 - \omega^2/\omega_{0i}^2 + 1.5 B(k) \omega^2 / D(k,\omega),$$

$$B(k) = 1 + 3(m_e/m_i) n_e \nu_{ei} / (k^2 \kappa_{e0}),$$

$$A(k) = n_e/(k^2 \kappa_{e0}) + (4/3) \eta_{i0} / (n_e T),$$

$$D(k,\omega) = (3\omega/2)^2 + b(k)^2, \ \omega_{0i} = k(T/m_i)^{1/2},$$

$$b(k) = k^2 \kappa_{i0}/n_e + 3(m_e/m_i) \nu_{ei}.$$

$$\kappa_{e0} = 3.14 n_e v_{Te}^2 / \nu_{ei}$$

$$\kappa_{i0} = 3.91 n_i v_{Ti}^2 / \nu_{ii}$$

$$\eta_{i0} = 0.96 n_i T_i / \nu_{ii}$$

Onsager's hypothesis

Fluctuations of dynamical quantities evolve in accordance with the same model equations as those governing macroscopic processes. Thus, for example, fluctuations on hydrodynamical scale relax due to collisions according to the equations of linearized hydrodynamics. Or linearized kinetic equation provides description over full range of scales and frequencies.

We used nonlocal, nonstationary hydrodynamics to evaluate correlation function of electron density fluctuations (cf. W. Rozmus *et al*. Phys. Rev. **E96**, 043207 (2017)). Our nonlocal hydro model is equivalent to the solution of linearized kinetic equation.

$$\frac{\partial \delta n_a}{\partial t} + n_a i k u_a = 0,$$

$$\frac{\partial u_a}{\partial t} = \frac{e_a}{m_a} E_a{}^* - \frac{1}{m_a n_a} ik\Pi_\parallel^a + \frac{1}{m_a n_a} R_{ab},$$

$$\frac{\partial \delta T_a}{\partial t} + \frac{2}{3n_a} ikq_a + \frac{2}{3} T_a i k u_a = 0,$$

$$S(k,\omega) = \frac{\langle \delta n_e^2 \rangle_{k,\omega}}{n_e} = \frac{1}{n_e} \int d^3\rho \int d\tau e^{i\omega\tau - i\vec{k}\cdot\vec{\rho}} G_{ee}(\vec{\rho},\tau)$$

$$G_{ab}(\vec{\rho},\tau) = \langle \delta n_a(\vec{r},t)\delta n_b(\vec{r}',t') \rangle$$

$$\vec{\rho} = \vec{r} - \vec{r}' \text{ and } \tau = t - t'$$

$$E_a^* = E - ik(\delta n_a T_a + n_a \delta T_a)/(e_a n_a)$$

$$q_e = -\frac{\alpha T_e}{\sigma} j - \kappa_e ik\delta T_e - n_e T_e \beta u_i,$$

$$E_e^* = \frac{j}{\sigma} - \frac{\alpha}{\sigma} ik\delta T_e - \frac{\beta_j}{\sigma} e n_e u_i,$$

$$\mathcal{R}_{ie} = -\frac{(1-\beta_j)}{\sigma} enj + \left(\beta + \frac{e\alpha}{\sigma}\right) ikn_e\delta T_e + \left(\frac{e^2 n_e \beta_j (1-\beta_j)}{\sigma} - m_e \beta_r \nu_{ei}^T\right) n_e u_i,$$

$$q_i = -\kappa_i ik\delta T_i - \beta_i n_i T_i u_i, \quad \Pi_\parallel = -4/3 ik\eta_i u_i - \beta_i n_i \delta T_i,$$

The only input required to find dynamical form factor is static correlation function

$$G_{ab}(k,0) = \langle \delta n_a(k,0)\delta n_b(-k,0) \rangle$$

Laser induced density fluctuations

Incoherent lasers & enhanced fluctuations

Laser pulses of finite temporal and spatial bandwidth are used in ICF experiments and employed as TS probes. The effect of the laser pulse incoherence on the TS cross-section has been quantified and it leads to broadening of the scattering spectra. Such pulses can have also direct effect of the level of ion acoustic fluctuations.

Density fluctuations driven by the ponderomotive force:

$$\frac{\partial^2 \delta n}{\partial t^2} + 2\gamma_a \frac{\partial \delta n}{\partial t} - c_s^2 \Delta \delta n = -\frac{c_s^2}{2} \frac{n_e}{n_c T_e} \Delta I$$

Laser with hot spots and time smoothing – spectral density $\langle I^2 \rangle_{\omega,k}$ produces density fluctuations such that the spectral density reads:

$$\left\langle \frac{\delta n^2}{n_e^2} \right\rangle_{\omega,\mathbf{k}} = \left| \frac{1/2}{(\omega/kc_s)^2 + 2i\gamma_a \omega/kc_s^2 - 1} \right|^2 \frac{\langle I^2 \rangle_{\omega,\mathbf{k}}}{n_c^2 T_e^2}$$

$$\langle \delta n_e^2 \rangle^{1/2} / n_e \sim (kc_s/\gamma_a)^{1/2} (I_0 / n_c T_e)$$

where the laser bandwidth $\geq kc_s$

For electron Landau damping one has level of fluctuations $\sim (m_i/m_e)^{1/4} (I_0/n_c T_e)$

The average laser intensity

$$\int \frac{d\omega}{2\pi} \frac{d^3\mathbf{k}}{(2\pi)^3} \langle I^2 \rangle_{\omega,\mathbf{k}} = I_0^2$$

$$\langle I^2 \rangle_{\omega,\mathbf{k}} = \frac{\pi}{k_\perp a_0} I_0^2 V_{HS} \tau_0 \exp\left[-\frac{1}{4}\omega^2 \tau_0^2 - \frac{1}{4} k_\perp^2 a_0^2 - \left(k_z - \frac{\omega}{v_g} \right)^2 \frac{L_R^2}{k_\perp^2 a_0^2} \right], \quad V_{HS} = 2\pi a_0^2 L_R$$

Thermal response

For parameters of experiment: n_e=7 10^{19} cm^{-3}, T_e=850 eV, T_i=190 eV, Z=15 collisions are important: $\lambda_{ei}=13\ \mu\mathrm{m}, \lambda_{ii} = 1.56\ 10^{-2}\mu\mathrm{m}$, i.e. on the scale of speckle collisions will change (enhance) the level of density fluctuations. Use nonlocal hydrodynamics. (Brantov *et al*. Phys. Plasmas **6**, 3002 (1999)).

$$\left\langle \frac{\delta n_e^2}{n_e^2} \right\rangle_{\omega,\mathbf{k}} = |D^N(\omega,k)|^2 \frac{\langle I^2 \rangle_{\omega,\mathbf{k}}}{n_c^2 T_e^2}, \qquad D^N(\omega,k) = \frac{A_k}{(\omega/kc_s)^2 + 2i\gamma_a\omega/k^2c_s^2 - (v_s/c_s)^2},$$

$$\gamma_a = \frac{2k^2 v_{Ti}^2}{3\nu_i}\mathrm{Re}\ \eta_i + \nu_{ei}^T \frac{c_s^2}{2v_{Te}^2}\beta_u + c_s^2 n_e \frac{(1-\beta)^2}{2\kappa} \qquad A_k = \frac{1}{2} + \xi_u + \frac{n_e v_{Te}\lambda_{ei}}{\kappa}(1-\beta)\left(\frac{1}{k^2\lambda_{ei}^2} + \xi\right)$$

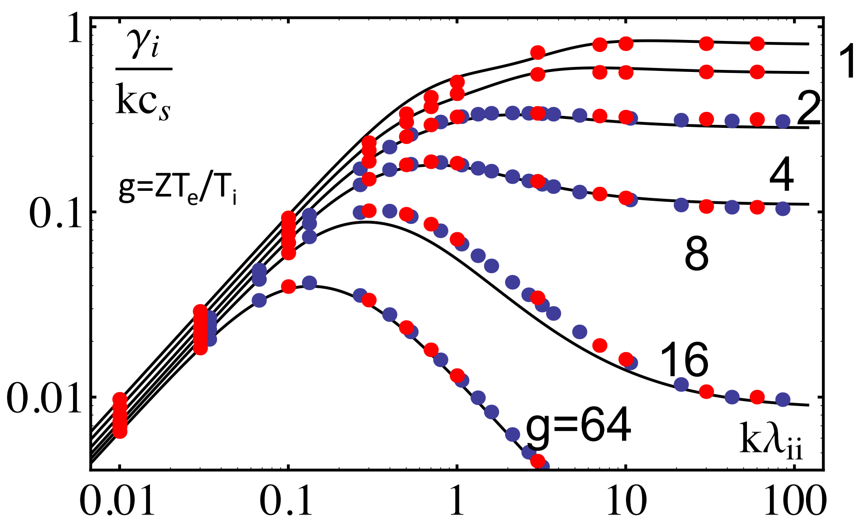

Approximately, for the parameters of the experiment the coupling coefficient

$$A_k \approx \tfrac{1}{2} + 0.88 Z^{5/7}(k\lambda_{ei})^{-4/7}$$

can produce order of magnitude enhancement above ponderomotive coupling level

Even for no frequency bandwidth TS may probe enhanced fluctuations by the laser

Nonequilibrium distribution functions

Heat flux and return current

Electron distribution function for the Spitzer-Härm transport model

$$f_e^{SH}(\vec{v}) = f_0^M(v) + \mu f^{SH}{}_1(v), \quad f^{SH}{}_1(v) = \frac{1}{3}\sqrt{\frac{2}{\pi}}\frac{\lambda_{ei}}{L_T}\frac{v^4}{v_{Te}^4}\left(4 - \frac{v^2}{2v_{Te}^2}\right)f_0^M(v), \quad \frac{1}{L_T} = \left|\vec{\nabla}\ln T_e\right|$$

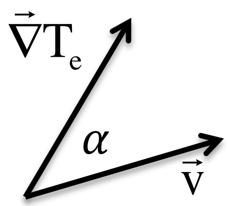

$\mu=\cos(\alpha)$

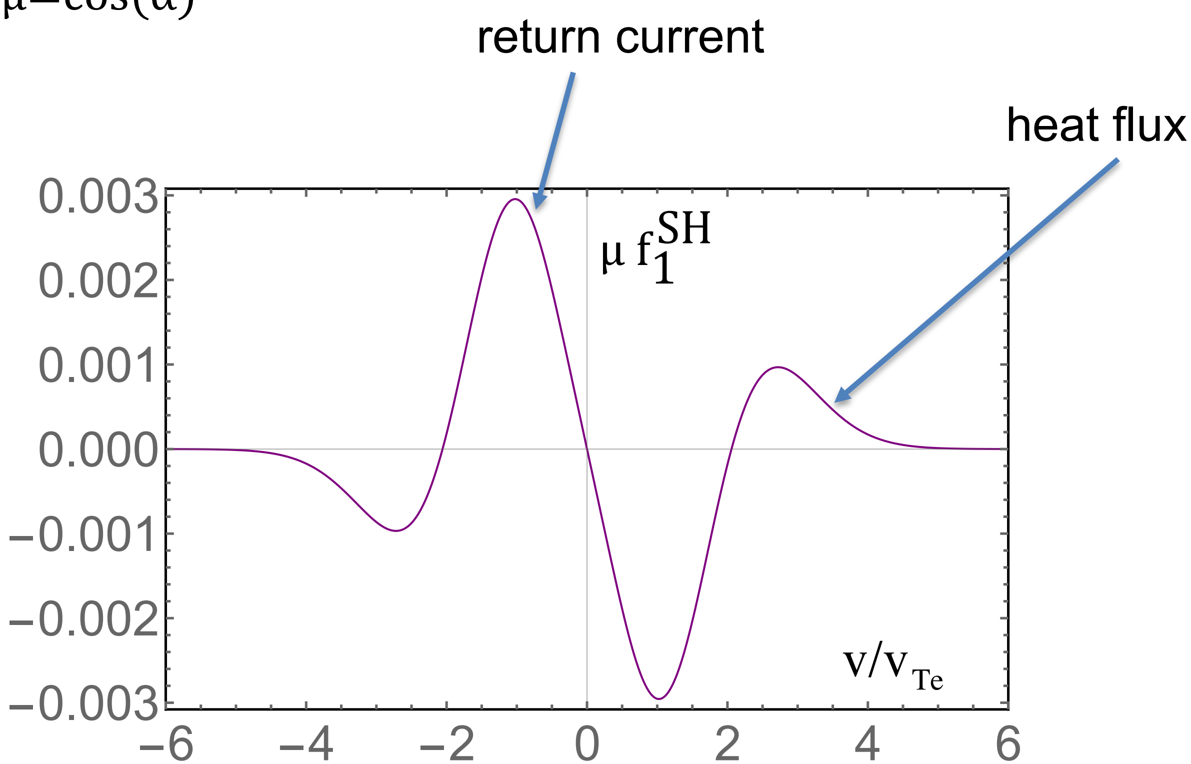

$$\delta_T = \frac{\lambda_{ei}}{L_T}$$

Thermal transport

Electron heat flux is poorly described by the classical diffusive model, $q_{SH}=-\kappa\nabla T_e$, in many laser produced plasmas. Thermal transport requires kinetic theory or nonlocal closure when reduced to hydrodynamical description.

PHYSICAL REVIEW LETTERS **121**, 125001 (2018)

Observation of Nonlocal Heat Flux Using Thomson Scattering

R. J. Henchen,[1,2,*] M. Sherlock,[3] W. Rozmus,[4] J. Katz,[1] D. Cao,[1] J. P. Palastro,[1] and D. H. Froula[1,5]

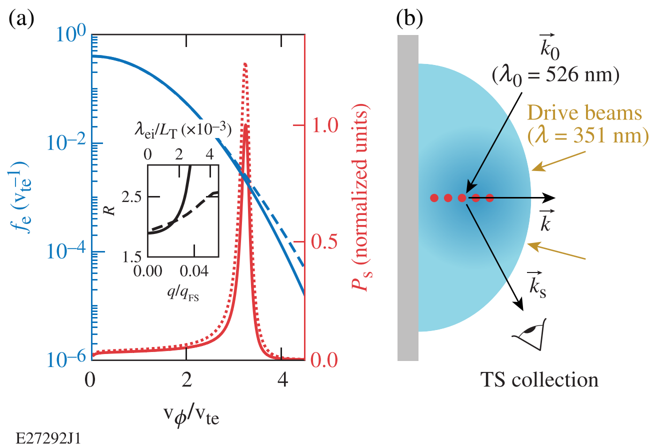

FIG. 1. (a) Calculated Thomson-scattering features (red curve, right axis) from electron plasma waves [Eq. (1)] are shown ($v_\phi = \omega/k$) using a Maxwellian (solid blue curve, left axis) electron distribution function and the non-Maxwellian (dashed blue curve) distribution that accounts for classical SH heat flux ($\lambda_{ei}/L_T = 2.2\times10^{-3}$, $q/q_{FS} = 3\%$). Inset: For a fixed normalized phase velocity, the ratio (R) of the peak scattered power of the up- and downshifted features are shown for calculations that use classical SH (solid curve, top axis) and nonlocal (dashed curve, bottom axis) distribution functions over a range of heat flux. (b) A schematic of the setup is shown.

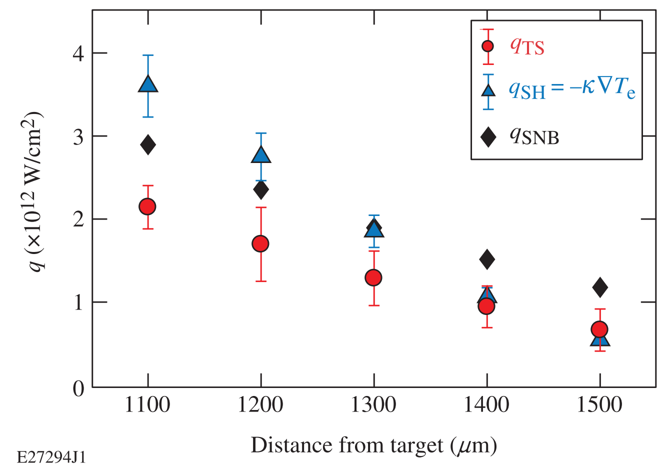

- Asymmetry of resonances associated with electron plasma waves propagating with and against the heat flux in $S(\vec{k},\omega)$ is used to measure q_{TS} by employing results of Vlasov-Fokker-Planck simulations.
- SNB is G. Shurtz, Ph. Nicolai, M. Busquet, Phys. Plasmas **7**, 4238 (2000) – current standard in nonlocal transport implementation into radiation hydrodynamics.

TS from high-Z laser plasmas

VOLUME 82, NUMBER 1 PHYSICAL REVIEW LETTERS 4 JANUARY 1999

Thomson Scattering from High-*Z* Laser-Produced Plasmas

S. H. Glenzer,[1] W. Rozmus,[2,*] B. J. MacGowan,[1] K. G. Estabrook,[1] J. D. De Groot,[1,3] G. B. Zimmerman,[1]
H. A. Baldis,[2] J. A. Harte,[1] R. W. Lee,[1] E. A. Williams,[1] and B. G. Wilson[1]
[1] *L-399, Lawrence Livermore National Laboratory, University of California, P.O. Box 808, Livermore, California 94551*
[2] *Institute for Lasers Science Applications, University of California, Livermore, California 94550*
[3] *Department of Applied Science and Plasma Research Group, University of California, Davis, California 95616*
(Received 30 September 1998)

We present the first simultaneous observations of ion acoustic and electron plasma waves in laser-produced dense plasmas with Thomson scattering. In addition to measuring the standard plasma parameters, electron temperature and density, this novel experimental technique is shown to be a sensitive method for temporally and spatially resolved measurements of the averaged ionization stage of the plasma. Experiments with highly ionized gold plasmas clearly show that the inclusion of dielectronic recombination in radiation-hydrodynamic modeling is critically important to model cooling plasmas. [S0031-9007(98)08073-9]

- Simultaneous fits to ion acoustic and electron plasma fluctuations are standard in TS experiments.
- Here ZT_e is well approximated by the ion acoustic peaks separation ($ZT_e \gg T_i$).
- Inclusion of dielectronic recombination in radiation-hydrodynamic modeling of Au plasma was croical for the correct modeling of this plasma.

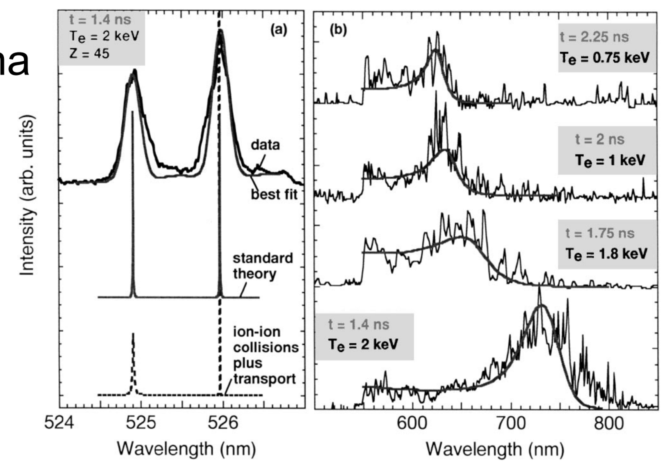

FIG. 2. Measured ion (a) and electron (b) feature of the Thomson scattering spectrum along with theoretical fits.

Laser heated electron distribution functions

E. Fourkal, *et al.* Phys. Plasmas **8**, 550 (2001)

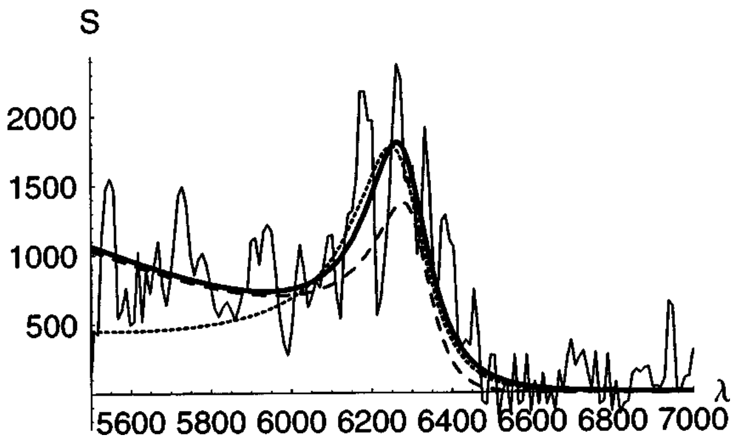

FIG. 6. The electron plasma wave fluctuation spectra (in arbitrary units) as a function of the scattered light wavelength in Å. Experimental data (noisy solid line) is taken from Ref. 6 and corresponds to the measurement at $t = 2.25$ ns. A Maxwellian fit ($T_e = 750$ eV, $n_e = 5.5\times 10^{19}$ cm^{-3}) is given by a dotted line. The dashed line shows a fit with the super-Gaussian EDF (11) and the solid line corresponds to the spectrum calculated with a new non-Maxwellian EDF (13) for the following plasma parameters $m=4$, $n_e = 4.5\times 10^{19}$ cm^{-3}, $T_e = 950$ eV, $Z = 26$.

- For the parameter $\alpha = Zv_0^2/v_{Te}^2 > 1$, e-e collisions are not frequent enough to restore Maxwellian in the bulk of electrons.
- Collisional absorption of the laser light ($v_0 = eE/m\omega$) results in super-Gaussian distribution functions:

$$\phi(x) = \phi_0 e^{-(x/x_0)^m} = 3\sqrt{\frac{\pi}{2}}\frac{m\Gamma(5/m)^{3/2}}{(3\Gamma(3/m))^{5/2}} \times \exp\left[-\left(\frac{x}{x_0}\right)^m\right],$$

$$x_0 = \left(\frac{3\Gamma(3/m)}{\Gamma(5/m)}\right)^{1/2}, \quad m = 2 + \frac{3}{1+1.66/\alpha^{0.724}}$$

J.-P. Matte, et al. , Plasma Phys. Contr. Fusion, 1988

- Electron-electron collisions between bulk electrons and fast electrons from the tail will restore Maxwellian tails , albeit slowly. In inhomogeneous plasmas that are locally heated by the laser heat carrying electrons will repopulate the tails of the electron distribution function.

Laser heated electron distribution functions

Super Gaussian approximates isotropic part of the electron distribution function (EDF). Such EDFs do not exist in laser produced plasmas because of localized heating and tails of hot electrons, return current, non-isotropic pressure contributions, etc. cf. Brunner, Valeo, Phys. Plasmas **9**, 923 (2002); Batishchev *et al*. Phys. Plasmas **9**, 2302 (2002).

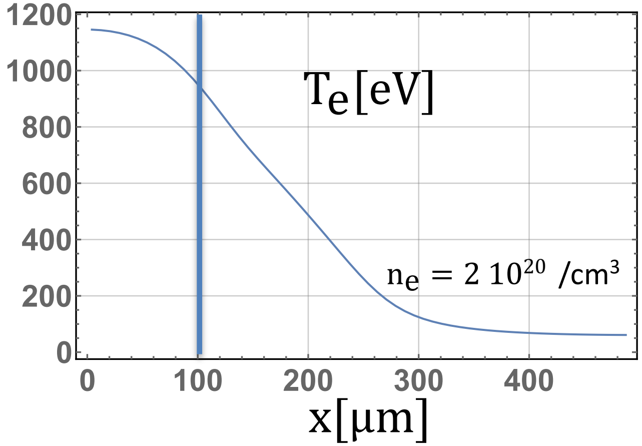

Profile of the temperature that overlaps with the laser pulse, with the max I=1.8 10^{15} W/cm^2 .

Simulate EDF at x=100 μm using K2 VFP code – M. Sherlock

EDFs are projected on the direction of $\overrightarrow{-\nabla T_e}||\vec{k}$ (of TS probed fluctuations)

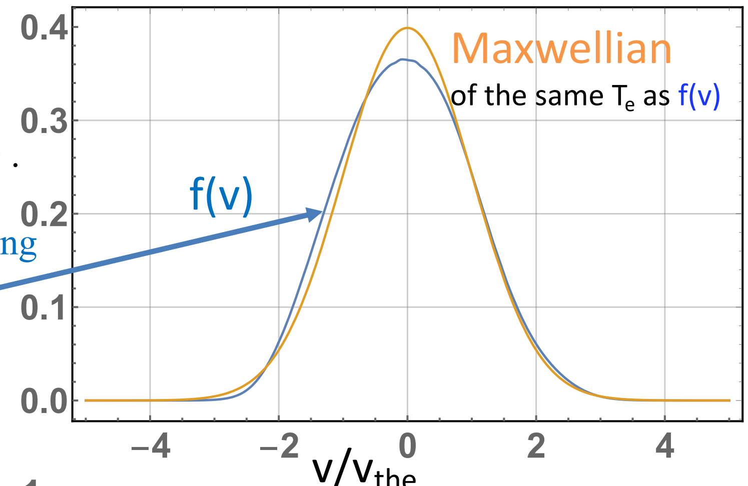

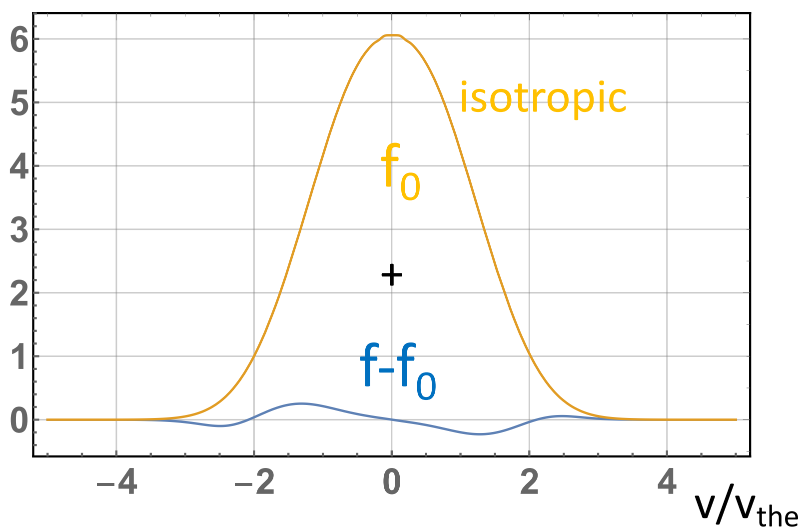

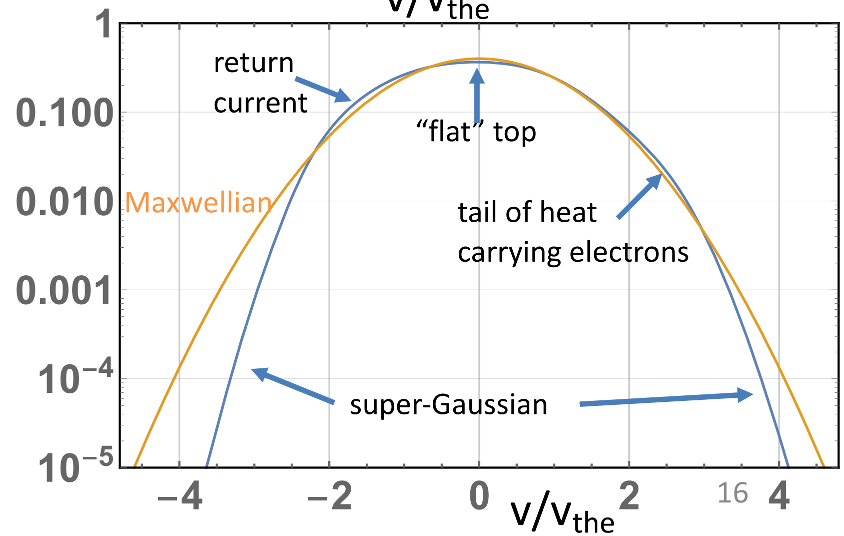

TS from laser produced plasmas

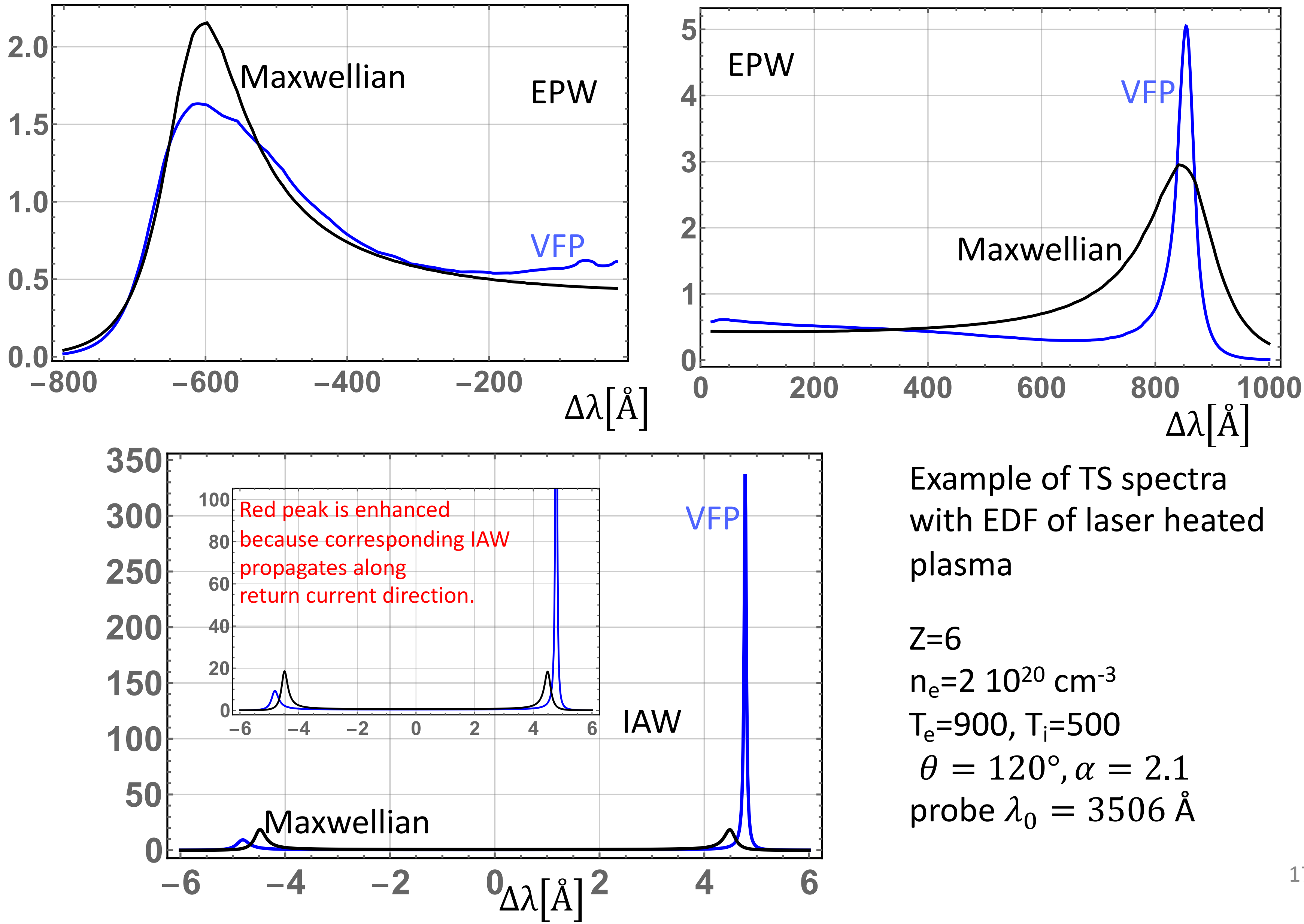

Example of TS spectra with EDF of laser heated plasma

Z=6
n_e=2 10^{20} cm^{-3}
T_e=900, T_i=500
$\theta = 120°, \alpha = 2.1$
probe $\lambda_0 = 3506$ Å

TS from laser produced plasmas

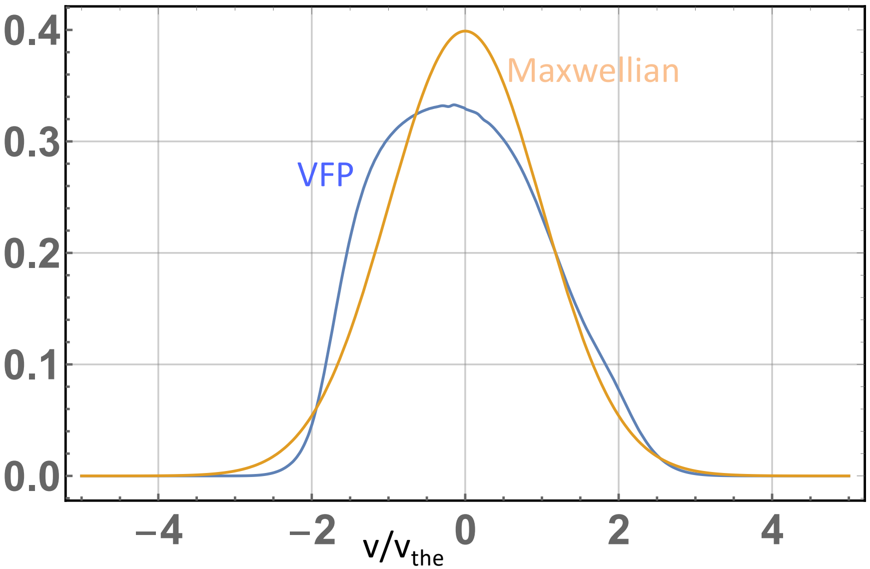

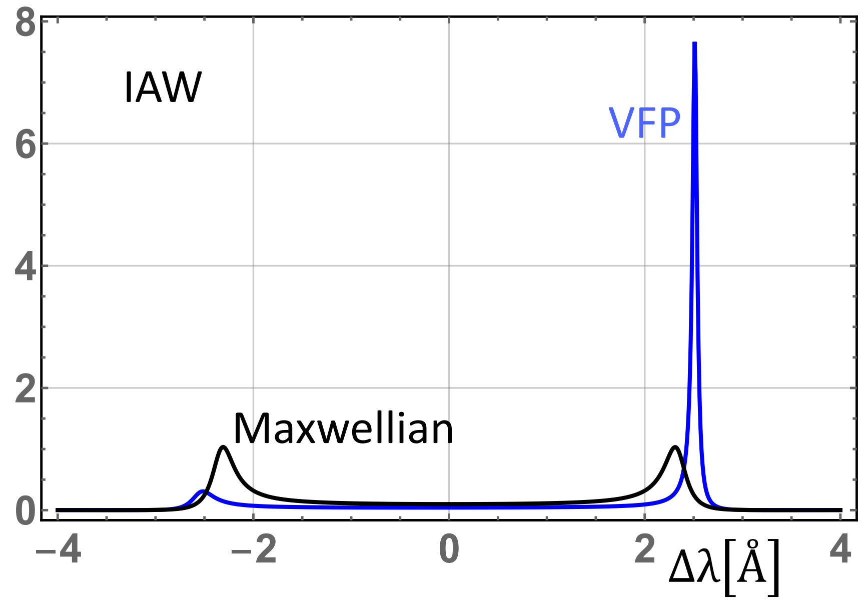

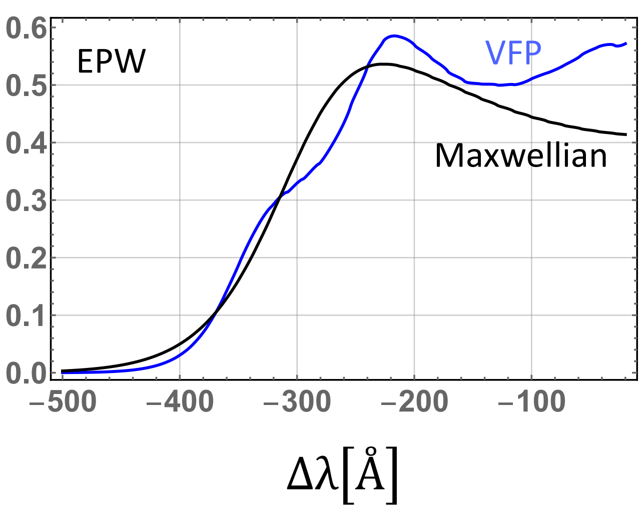

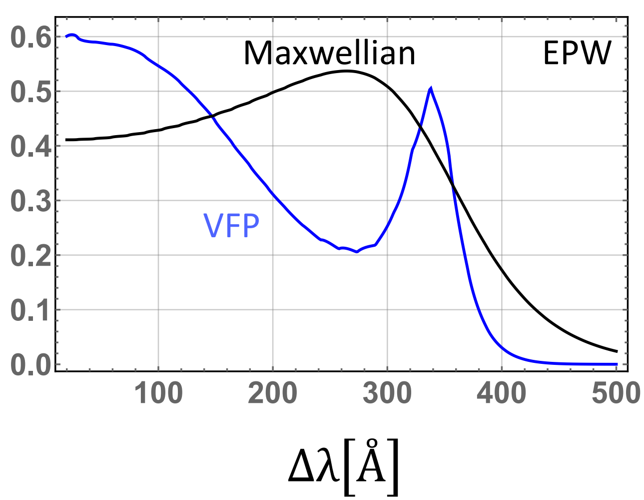

Example of TS spectra with EDF of laser heated plasma. Strongly driven plasma, $I=5\ 10^{15}$ W/cm^2

$Z=6$

$n_e=2\ 10^{19}$ cm^{-3}

$T_e=900$, $T_i=500$

$\theta = 60°, \alpha = 1.7$

probe $\lambda_0 = 3506$ Å

Plasma unstable with respect to electromagnetic instability

Magnetic field generation

Anna Grassi, Frederico Fiuza, SLAC, described by 2D particle-in-cell (PIC) simulations Weibel instability of interpenetrating plasmas, magnetic field generation and collisionless shock formation

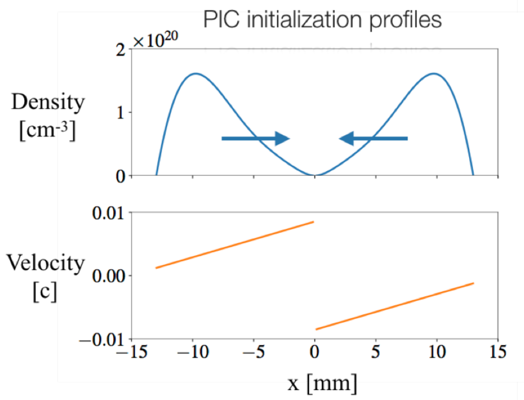

t=0.6 ns

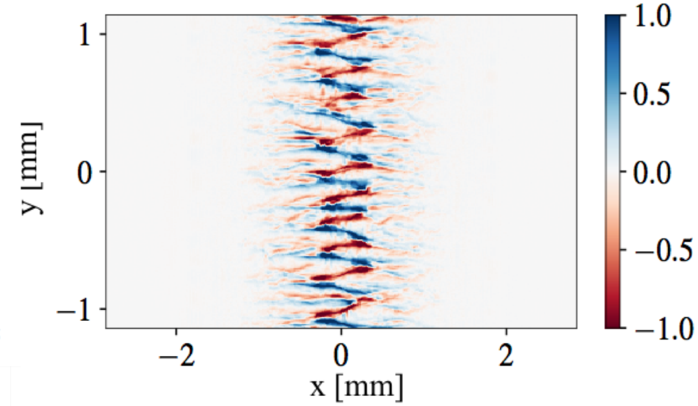

As a result of instability plasma flows are transversely modulated, give rise to current and B-field normal to the plane of simulations and shown at different times

t=1.2 ns

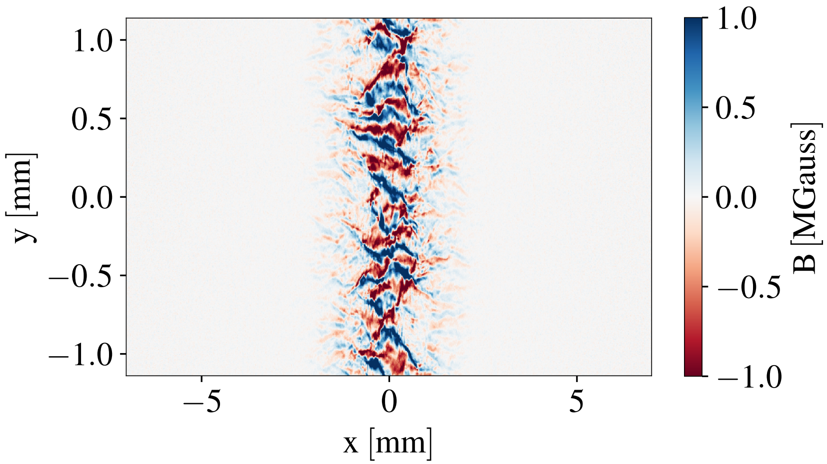

t=10 ns

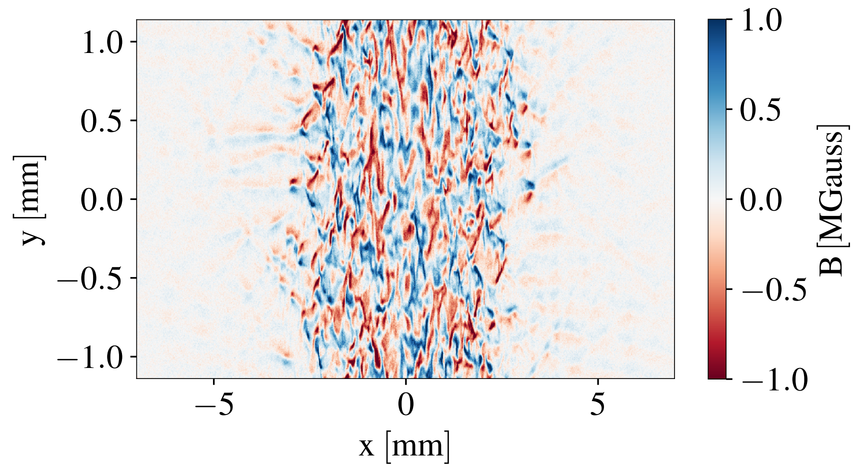

Magnetic field measurement by TS

C. Bruulsema, F. Fiuza, W.R., G. Swadling, S. Glenzer, propose local measurement of magnetic field in Weibel unstable plasmas. TS spectra are used to calculate electric current, and B-field, assuming that electron density fluctuations and $S(\vec{k},\omega)$ are not affected by the electromagnetic instability. The method is first validated by PIC simulations.

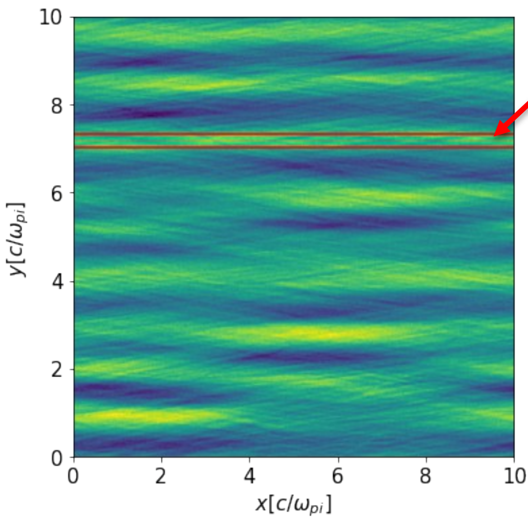

TS volume

Electric current in PIC simulations of the interpenetrating plasmas

Comparison of PIC current and results from "synthetic" TS

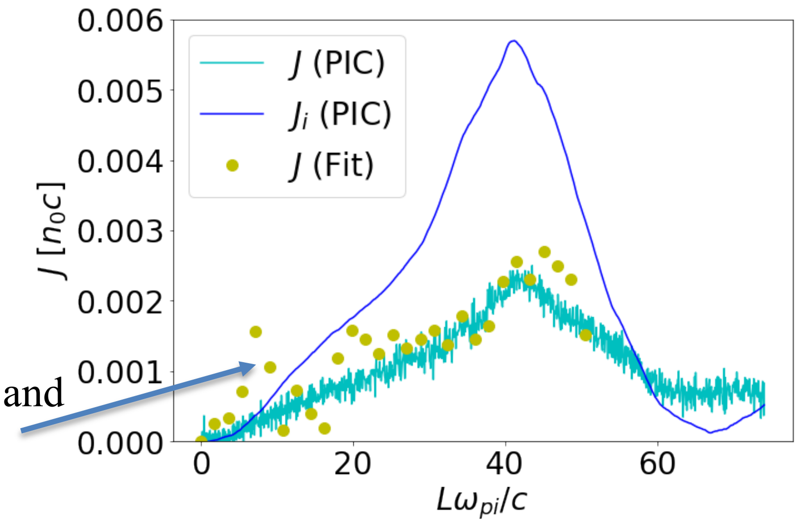

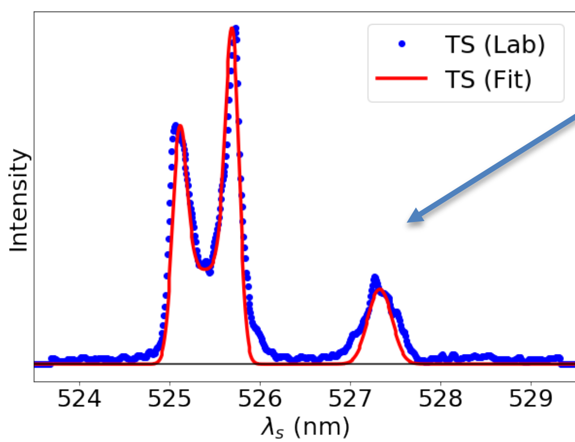

Sample of the experimental TS spectra and fits

Field strength from fit current

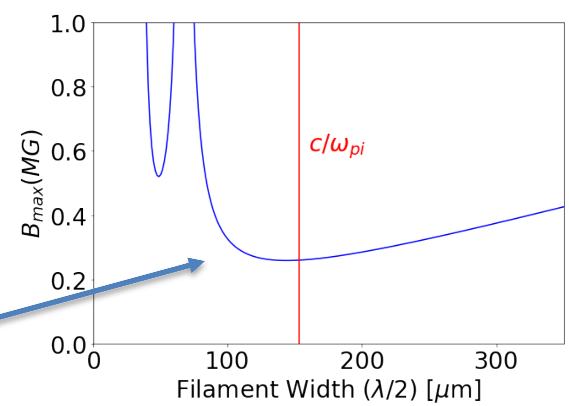

Ablative plasma profiles

The same analysis is repeated for the density and flow velocity profiles of the expanding plasmas, rather than periodic initially homogeneous flows.

Ion current in PIC simulations of the interpenetrating plasmas

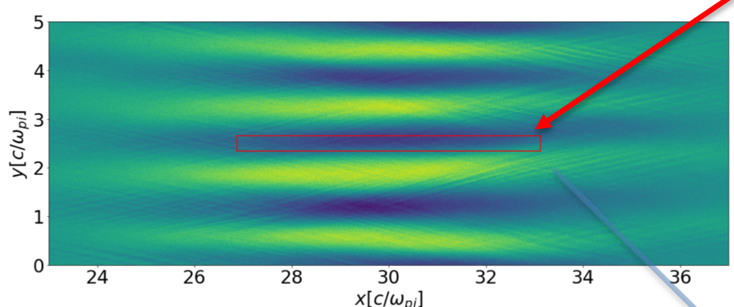

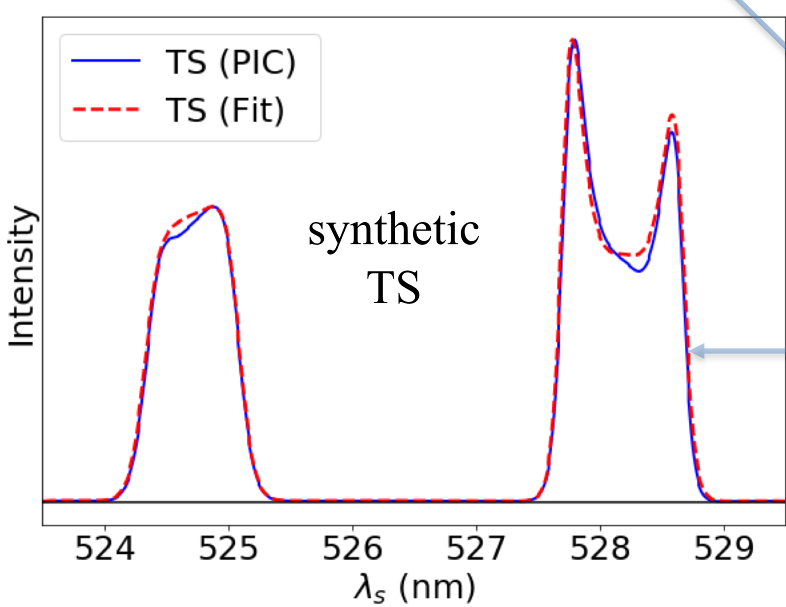

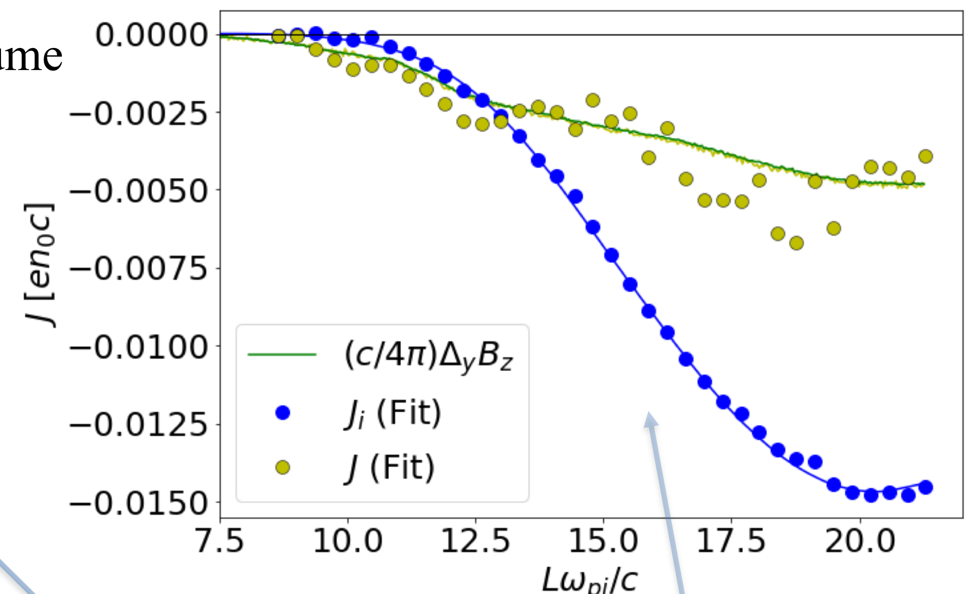

- Distributions functions are extracted from the TS volume in PIC simulations.
- Standard collisionless $S(\vec{k},\omega)$ is calculated using these distribution functions.
- Form factor is fitted with Maxwellians with several free parameters including "occupation" number.
- This allows evaluation of currents and B-fields.

Electrostatic turbulence

Unstable EPWs & TS

Nonlinear electron plasma waves driven by the stimulated Raman scattering undergo further decays that contribute to saturation of the scattering instability.

Phys. Plasmas **5** (1), January 1998

Time-resolved measurements of secondary Langmuir waves produced by the Langmuir decay instability in a laser-produced plasma

C. Labaune, H. A. Baldis,[a)] and B. S. Bauer[b)]
Laboratoire pour l'Utilisation des Lasers Intenses, Ecole Polytechnique, Centre National de la Recherche Scientifique, 91128 Palaiseau cedex, France

V. T. Tikhonchuk[c)] and G. Laval
Centre de Physique Théorique, Ecole Polytechnique, Centre National de la Recherche Scientifique, 91128 Palaiseau cedex, France

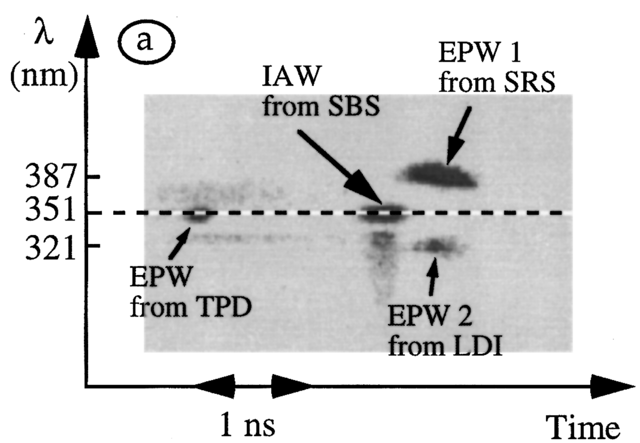

TS from enhanced electrostatic fluctuations and unstable plasmas

VOLUME 89, NUMBER 4 PHYSICAL REVIEW LETTERS 22 JULY 2002

Langmuir Decay Instability Cascade in Laser-Plasma Experiments

S. Depierreux,[1,*] C. Labaune,[1] J. Fuchs,[1] D. Pesme,[2] V. T. Tikhonchuk,[3] and H. A. Baldis[4]

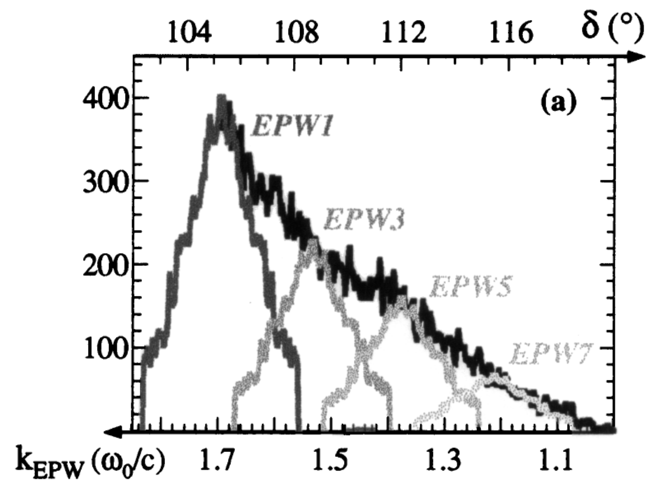

TS spectrum of epw cascade reconstructed from the experimental data using instrumental spectral width for each component of the cascade.

Return current instability (RCI)

Forslund, J. Geophys. Res. **75**, 17 (1970)

From the collisionless $(k \sim k_{De} \gg 1/\lambda_{ei})$ electron dispersion relation

$$\boxed{\gamma_e = \gamma_s(-1+p_T)\,, \quad p_T = \frac{kv_{Te}}{\omega}\cos\theta\,\frac{(2\pi)^{3/2}v_{Te}^2}{n_e}\int_0^\infty dv\, f_1(x,v)\,, \quad \gamma_s = \sqrt{\frac{\pi}{8}}\frac{\omega^4}{k^3c_s^3}\frac{\omega_{pi}}{\omega_{pe}}\,,}$$

Using $f_1=f_1^{SH}$:

$$p_T^{SH} = \frac{kv_{Te}}{\omega}\cos\theta\,\frac{3}{2}\xi_\gamma(Z)\delta_T, \qquad \xi_\gamma = \frac{Z+0.5}{Z+2.12}\,,$$

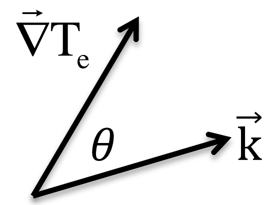

In a high Z plasma (e.g. Au) i-i collisions are important for the IAW dispersion and damping, $k \sim 1/\lambda_{ii}$,

$$k_i = k\lambda_{ii},\; r = g/(1+k^2\lambda_{De}^2),\; g = ZT_e/T_i.$$

$$\frac{\omega}{kv_{Ti}} = \sqrt{r + \frac{5}{3} + Q\left(r,k_i\right)\left(G\left(r\right) - \frac{5}{3}\right)},$$

$$Q(r,k_i) = \frac{r^{3/2}k_i^2 + k_i\sqrt{r}}{r^{3/2}k_i^2 + 3k_i\sqrt{r}+10}\,, \qquad G = \frac{3r^3+11r^2+12}{r^3+7r}\,.$$

$$R^{-1} = 1 + \left[rk_i^2(0.05r+0.04)\right]^{-1}$$

$$\frac{\gamma_i^H}{kv_{Ti}} = k_i\frac{r+3.02}{r+1.67}\,\frac{0.80rk_i^2+1.49}{r^2k_i^4+4.05rk_i^2+2.33}\,.$$

$$\frac{\gamma_i^L}{kv_{Ti}} = \sqrt{\frac{\pi}{8}}r^2\exp\left[-\frac{r}{2}-\frac{G(r)}{2}\right]\frac{10+21r+r^3}{2r^2+r^3}\,.$$

$\gamma = \gamma_e - \gamma_i, \;\; \gamma_i = \gamma_i^H + R(k_i,r)\,\gamma_i^L$

cf. Brantov *et al*. Phys. Rev. Lett. **108**, 205001 (2012), and Bychenkov, et al. Phys. Plasmas **1**, 2419 (1994).

Ion-acoustic turbulence

- Influential monograph *Plasma Turbulence* by B.B. Kadomtsev was published in 1965 in English translation. It addressed not only quasi-linear and weak-turbulence theory but also sophisticated results about strong turbulence.
- Eq. (IV.18) from Kadomtsev's book describes evolution of the ion acoustic turbulence in terms of the spectral intensity I_k according to weak turbulence theory:

$$\frac{\partial I_k}{\partial t} - \frac{1}{k^2}\frac{\partial}{\partial k}\left(Ak^7 I_k^2\right) = 2\gamma_k I_k - Ak^4\, I_k^2,$$ giving stationary solution: $$\boxed{I_k = \frac{\alpha}{2Ak^3}\ln\frac{k_0}{k}}$$

where the linear growth rate of the ion acoustic instability, $\gamma_k = \alpha k$.

- This result has been refined and generalized, cf. V.Yu. Bychenkov, *et al*. Physics Reports **164**, 119 (1988). Subsequently several attempts have been made to incorporate it into main stream laser plasma interaction theory.

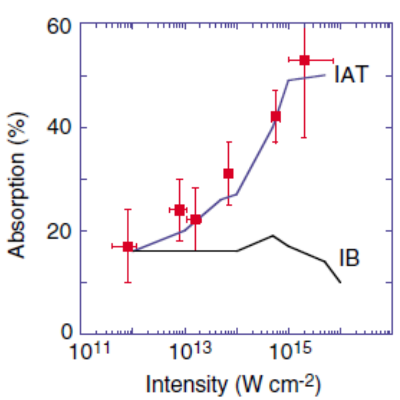

FIG. 4 (color). Absorption for various 2ω probe beam intensities. The comparison with two models show that inverse bremsstrahlung absorption (IB) is not sufficient to explain the measurements (squares). Good agreement can be seen when including ion acoustic turbulence (IAT).

VOLUME 88, NUMBER 23 PHYSICAL REVIEW LETTERS 10 JUNE 2002

Anomalous Absorption of High-Energy Green Laser Light in High-Z Plasmas

S. H. Glenzer,[1] W. Rozmus,[2,3] V. Yu. Bychenkov,[4] J. D. Moody,[1] J. Albritton,[1] R. L. Berger,[1] A. Brantov,[4] M. E. Foord,[1] B. J. MacGowan,[1] R. K. Kirkwood,[1] H. A. Baldis,[2] and E. A. Williams[1]

Ion acoustic turbulence (IAT) contributes to anomalous collision frequency that enhances absorption of laser light as compared to classical inverse bremsstrahlung (IB) mechanism. No direct observation of IAT spectra has been made.

Stationary spectrum of IAT

Bychenkov, Silin, Uryupin, Phys. Reports 164, 119 (1988)

$$N(\vec{k}) = N(k)\Phi(x), \;\; x = \hat{n}\cdot \vec{k}/k$$

$$\vec{R} \equiv \hat{n}R = en_e\vec{E}_a - \vec{\nabla}\left(n_e T_e\right),$$

$\vec{E}_a$ – ambipolar field calculated from the zero current condition ~ $\vec{\nabla} T_e$

From the weak turbulence theory:

$$\text{Kadomtsev} - \text{Petviashvili} \quad (k\lambda_{De} < 1) : N(k) \propto k^{-4}\ln(1/k\lambda_{De})$$

$$\text{Galeev - Sagdeev} \quad (k\lambda_{De} > 1) : \quad N(k) \propto k^{-13}$$

$$\frac{N(k)}{4\pi n_e T_e} = \omega_{pi}\sqrt{\frac{\pi}{8}}\frac{ZT_e}{T_i}\frac{\lambda_{De}^3}{\omega_{pe}}W(y), \;\; y = k\lambda_{De}$$

$$W(y) = \frac{1}{y^3(1+y^2)^2}\left[\ln\frac{\sqrt{1+y^2}}{y} - \frac{1}{2(1+y^2)} - \frac{1}{4(1+y^2)^2}\right]$$

Angular Dependence

$$\nu^R_{\parallel,\perp} = \nu^R \mu_{\parallel,\perp}\,,$$

$$\nu^R = \frac{\omega_{pe}^2}{\omega_0}\int_{k_{min}}^{\infty} k^2 dk\, \frac{\omega_s(k)N(k)}{4\pi^2 n_e T_e}\,\frac{\epsilon_l''(\omega_0,k)}{|\,\epsilon_l(\omega_0,k)\,|^2}\,, \qquad k_{min} = max\{k_{ii}, k_0\}\,,$$

$$\mu_\parallel = \int_0^1 dx x^2 \Phi(x)\,, \quad \mu_\perp = \frac{1}{2}\int_0^1 dx(1-x^2)\Phi(x)\,, \qquad K_N = \frac{6\pi\omega_{pe}^2\lambda_{Di}^2 R}{\omega_{pi}^2 \lambda_{De} n_e T_e}$$

typically : $k_{min}\lambda_{De} \ll 1$

$$\mu_\parallel \simeq \frac{0.7}{\ln\left(K_N + 2.4/K_N\right)} + 1.1\sqrt{K_N}\,,$$

$$\mu_\perp \simeq \left(\frac{2.4}{K_N} + \frac{2.1}{\sqrt{K_N}}\right)^{-1}\,,$$

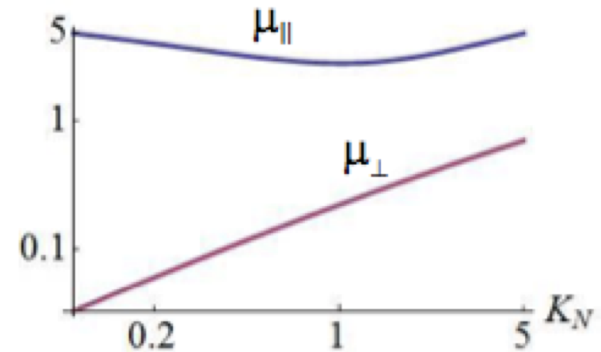

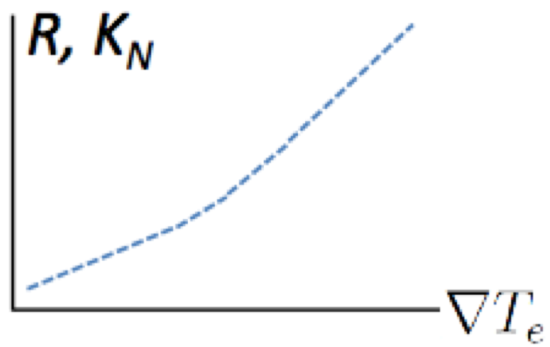

$$R \simeq 0.64 n_e \nabla T_e \qquad K_N \ll 1$$

$$R \simeq 1.5 n_e \nabla T_e \qquad K_N \gg 1$$

Classical & Anomalous Absorption

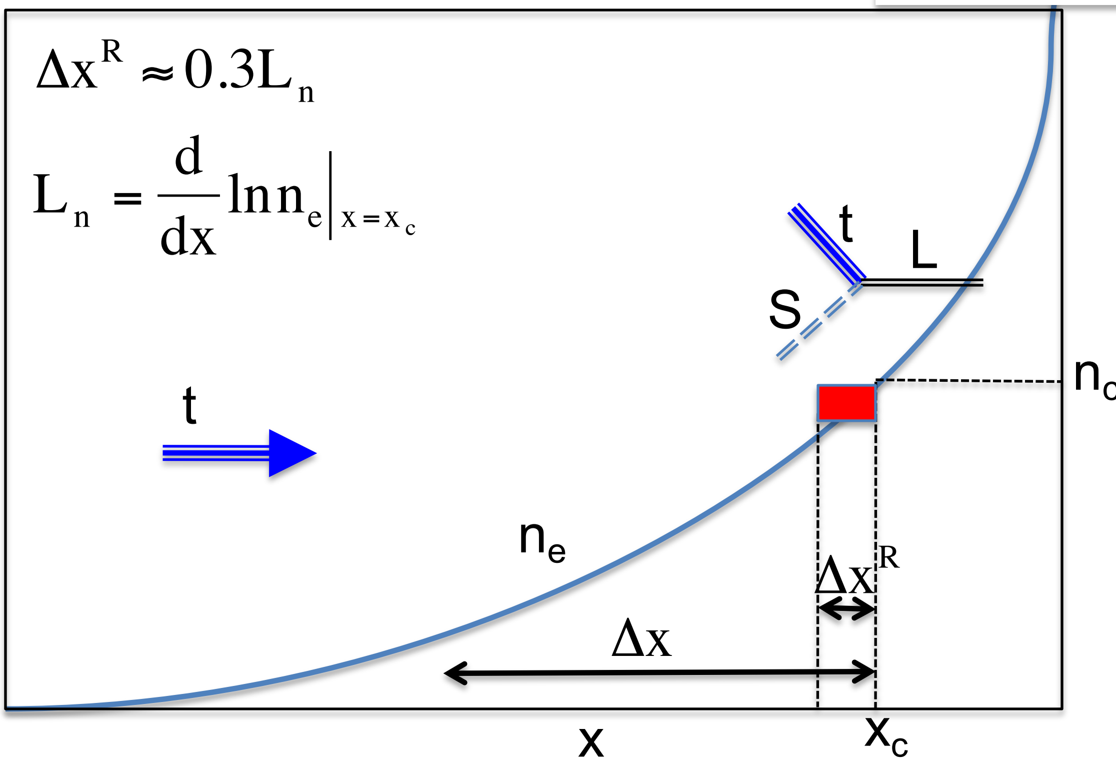

region	Classical	Anomalous
Δx	IB - Coulomb collisions, ν_{ei}	Enhanced collisions, ν_{an}
Δx^R	Resonance absorption	Resonance anomalous absorption, ν_{an}^R

Reduced model of IAT

Practical expressions for anomalous absorption and transport using Kadomtsev spectrum of the IAT have implemented in the radiation hydro codes (cf. M. Sherlock et al. 2017)

Linear threshold:

$$p_T^{SH}>1 \rightarrow \quad p_T^{SH} \approx \frac{3}{2}\frac{v_{Te}}{c_s}\frac{\lambda_{ei}}{L_T} > 1, \quad \text{nonlocal threshold: } p_T^{NL}>1$$

$$\text{small ion damping}: \quad \gamma_e = \gamma_s\left(p_T - 1\right) > \gamma_i$$

Knudsen number for IAT

$$K_N = \frac{6\pi\omega_{pe}^2\lambda_{Di}^2 R}{\omega_{pi}^2\lambda_{De} n_e T_e} \xrightarrow{J=0} 12\frac{T_i}{ZT_e}\frac{1}{m_e c_s \omega_{pi}}\left|\frac{\partial T_e}{\partial x}\right|$$

recall: $\vec{R} \equiv \hat{n}R = en_e\vec{E}_a - \vec{\nabla}\left(n_e T_e\right),$

Anomalous collision frequency

$$\nu_{an} = 0.04\,\omega_{pi}\frac{ZT_e}{T_i}\left(\frac{1+9K_N^2}{K_N^2+\ln^2\left(\frac{1}{K_N}\right)}\right)^{1/2}$$

Enhanced IB absorption

$$\kappa_{IB} = \frac{\nu_{ei}+\nu_{an}}{c}\left(\frac{n_e}{n_c}\right)\left(1-\frac{n_e}{n_c}\right)^{-1/2}$$

Au, $K_N \ll 1$

Anomalous heat flux

$$q_{an} = f n_e T_e v_{Te}, \quad f = 0.18\sqrt{\frac{Z}{A}}\left(1+1.6\sqrt{K_N}\right) \approx 0.09$$

Summary

- Thomson scattering from the particle noise – form factor, 1960, for stable, collisionless plasma not necessary in thermal equilibrium.
- Form factor with particle collisions from nonlocal and nonstationary hydrodynamics
- Enhanced fluctuation levels – thermal response to incoherent laser pulses
- Non-Maxwellian distribution functions – super Gaussians in laser heated plasmas, modified by thermal transport.
- Electromagnetic, Weibel unstable plasmas – laboratory astrophysics, measurement of the magnetic fields
- Langmuir and ion acoustic turbulence – enhanced fluctuation spectra, absorption, modified transport

Nonlocal transport regime

cf. Brantov et al. Phys. Plasmas **8**, 3558 (2001)

Naively, driving force of the RCI, according to SH theory, $p_T = p_T^{SH} \sim \delta_T$, thus by increasing δ_T one should enhance the RCI growth rate. Except for $\delta_T > 0.06/\sqrt{Z}$ SH is no more valid – transport is nonlocal and in the weak collision regime.,

Use nonlocal transport theory and $p_T = p_T^{NL}$:

$$p_T^{NL} = \frac{k v_{Te}}{\omega} \cos\theta \frac{3}{2} \xi_\gamma(Z) \delta_T^{NL}, \ \ \delta_T^{NL} = \frac{2}{3\xi_\gamma} \int \frac{dk'}{2\pi} e^{ik'x} \Gamma^T(k') \left[\frac{\lambda_{ei}}{T_e} \frac{dT_e}{dx} \right]_{k'}$$

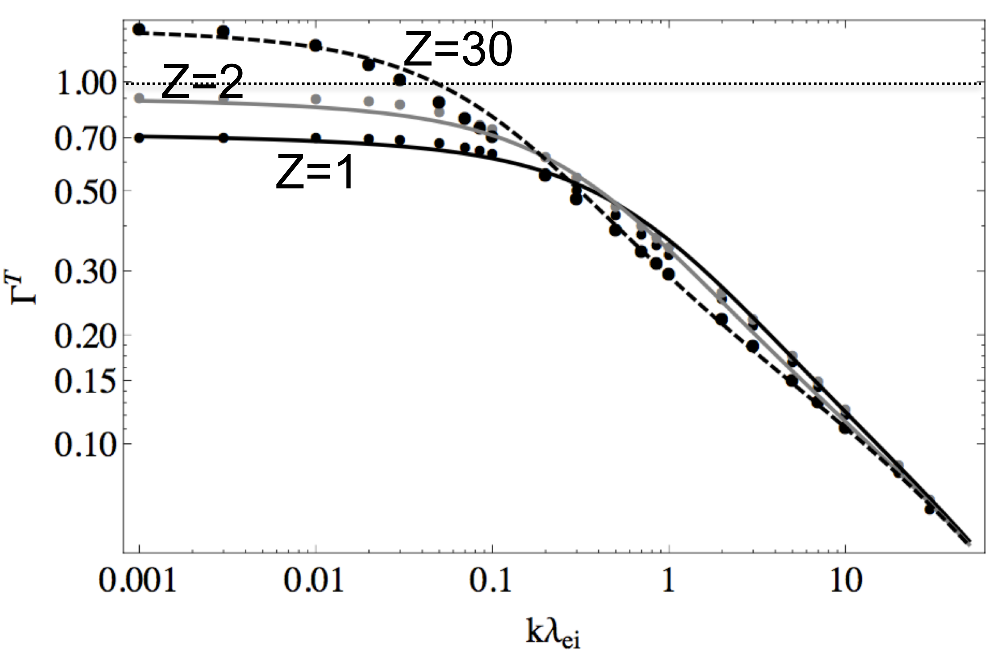

Fit to the nonlocal kernel $\Gamma^T(k)$:

$$\Gamma^T(x) = \frac{3}{2}\xi_\gamma \left(\frac{2}{3 + 30\xi_\gamma^3 x} + \frac{1}{3 + \xi_\gamma(4.5x^{0.35} + 0.18x)} \right)$$

for 1<Z<50 and $0 < k\lambda_{ei} < 100$ within 15% of the numerical solutions

Vlasov-Fokker-Planck simulations

Kinetic simulations of the ICF plasma on the local scale

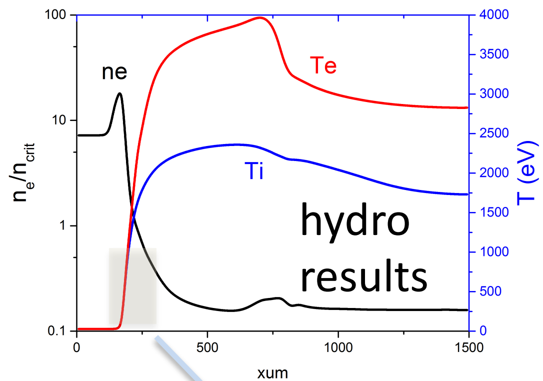

$$\frac{\partial f_e}{\partial t} + v_x \nabla f_e - \frac{e}{m_e}\vec{E}\cdot\frac{\partial f_e}{\partial \vec{v}} = C_{ei}[f_e, f_i] + C_{ee}[f_{e0}, f_{e0}],$$
$$\frac{\partial f_i}{\partial t} + v_x \nabla f_i + \frac{Ze}{m_i}\vec{E}\cdot\frac{\partial f_i}{\partial \vec{v}} = 0\,,$$

Profiles of modest, nonlocal gradients from VFP simulations

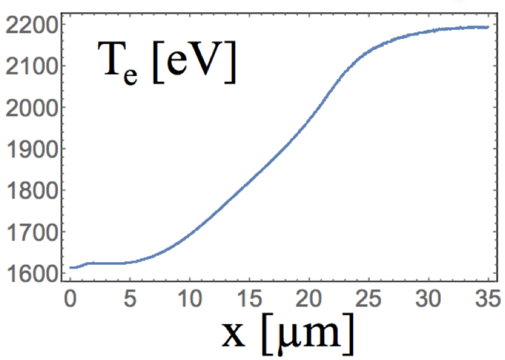

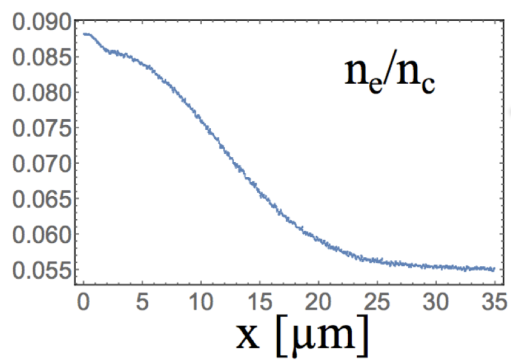

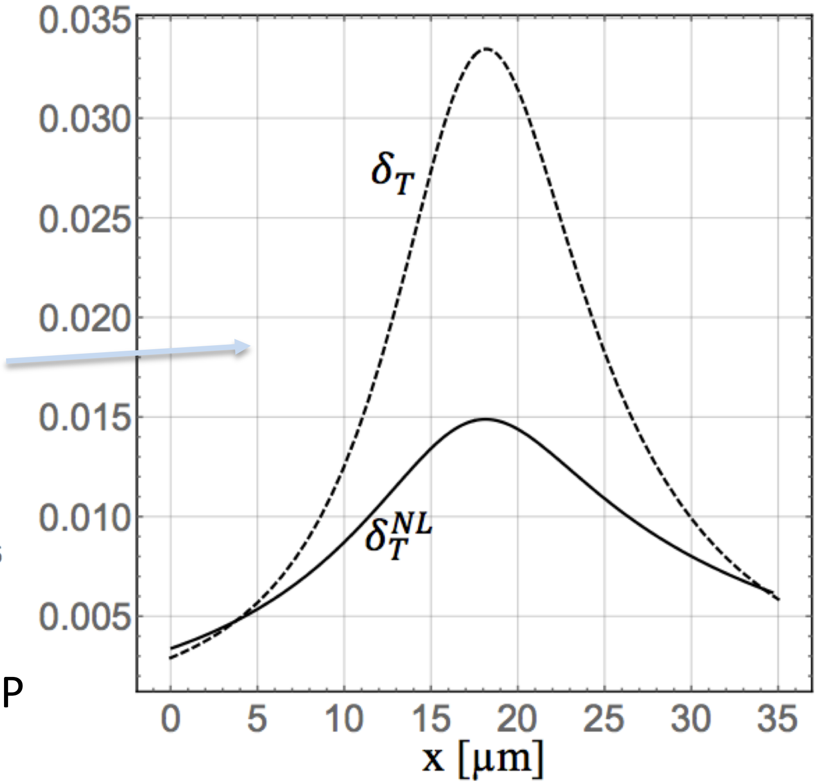

“Local” profiles in Au plasma (Z=50) at 10 ps from VFP code

VFP vs linear theory of RCI

For the profiles in Au plasma, growth rate calculations and comparison with VFP results

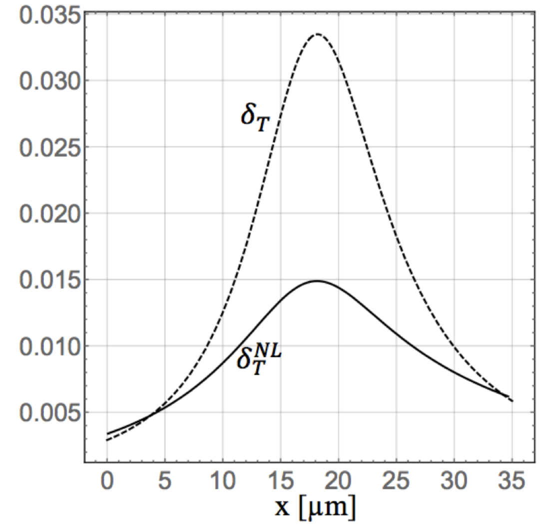

SH – Spitzer-Harm solution for f_1, using δ_T
VFP – growth rates from VFP simulations
NL1 – full nonlocal theory, using δ_T^{NL}
NL2 – as NL1 but without i-i collisions

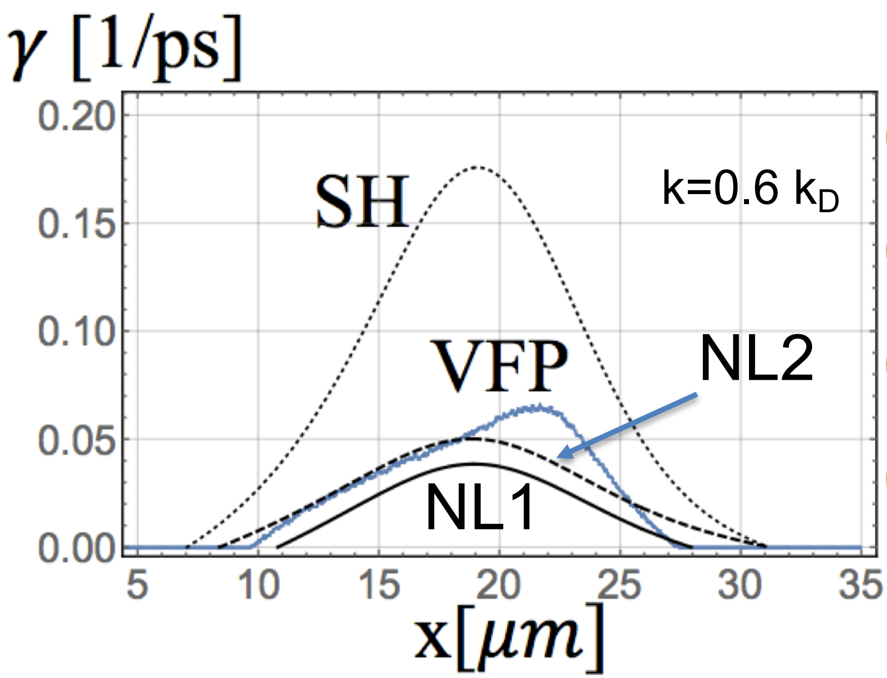

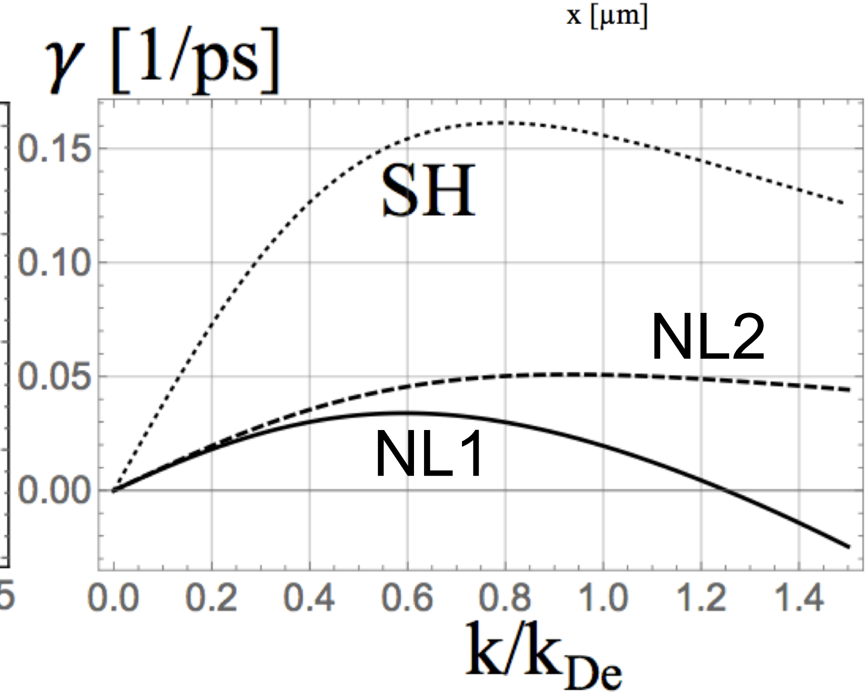

VFP simulations of RCI

For the profiles in Au (δ_T<0.035) the temporal evolution and spectra of IAT: